SpaceOps 2010 Conference
25-30 April 2010, Huntsville, Alabama

AIAA 2010-1928

Applications of Ultra-Low Ballistic Coefficient Entry Vehicles to Existing and Future Space Missions

David L. Akin*

Space Systems Laboratory, University of Maryland, College Park, MD 20742

The ballistic coefficient ($\beta = \frac{m}{c_D A}$) of entry vehicles has traditionally not been a design parameter: the mass was fixed by the launch vehicle payload, the drag coefficient was determined by the aerodynamic configuration, and the reference area (typically cross-section area) was fixed by the launch vehicle diameter. If the ballistic coefficient is instead considered as a potential design parameter, several benefits result from driving to lower and lower values. As the ballistic coefficient decreases, the peak stagnation point heating rate and temperature decrease. As β reaches the range of 150-300 Pa, the heat shield can be deployed using a mechanical framework (much like an umbrella) supporting existing ceramic fabric as the heat shield. Offsetting the center of gravity from the vehicle centerline allows lift/drag ratios in the range of 0.15-0.25, which mitigates entry decelerations and provides active targeting capability for a designated landing site. Due to the lower entry temperatures, ionization of the surrounding air stream is reduced or eliminated, allowing communications and GPS-based navigation throughout the entry trajectory. As the spacecraft enters the dense lower atmosphere, the low areal loading results in terminal velocities in the range of 15-20 m/sec, requiring only terminal decelerators (rockets or airbags) to mitigate the landing impact.

This paper reviews the concept and development history of ultra-low ballistic coefficient (ULβ) entry vehicles, as introduction to its focus on the applications of this class of vehicles to existing (ISS) and future (exploration) missions. Results are presented for the use of ULβ vehicles in future missions, including intact cargo down-mass from ISS and aerocapture and direct hypervelocity entry, descent, and landing (EDL) for lunar and Mars missions. Of particular interest is the potential for a ULβ-type vehicle as an alternate approach to crew transfer vehicles currently being developed under the NASA COTS program. Such a system offers several unique advantages over more conventional capsule or winged designs. The large wake area and relatively low airstream enthalpies allow the use of simple cylindrical shapes for the crew cabin, rather than the low volumetric efficiencies of conical configurations. Since the ParaShield itself supplies the capabilities for entry, descent, and landing, the EDL components of the spacecraft could be easily detached for lunar missions, allowing the ULβ crew cabin to be used for lunar landing and exploration missions while the deployable entry shield is parked in lunar orbit to reduce landed mass. Similar advantages accrue to a human Mars mission, including the use of ULβ for aerobraking into Mars orbit and direct hypervelocity EDL upon return to Earth from both the Moon and Mars.

Acronyms

AMROC	American Rocket Company
β	Ballistic Coefficient, $\frac{m}{c_D A}$
EDL	Entry, Descent, and Landing
EELV	Evolved Expendable Launch Vehicle
ESPA	EELV Secondary Payload Adapter
IRDT	Inflatable Reentry and Descent Technology
IRVE	Inflatable Reentry Vehicle Experiment

*Director, Space Systems Laboratory and Institute for Dexterous Space Robotics. Associate Professor, Department of Aerospace Engineering. Senior Member, AIAA

ISS	International Space Station
lb	Pounds (force)
LEO	Low Earth Orbit
MPLM	Mini Pressurized Logistics Module
SSL	Space Systems Laboratory
ULβ	Ultra-Low Ballistic Coefficient
UMd	University of Maryland

I. Introduction

In traditional entry vehicle design, the ballistic coefficient (β, defined as $\frac{m}{c_D A}$) has not been an independent variable in the systems design. The mass of an entry vehicle, such as the Apollo spacecraft, was fixed by the capacity of the launch vehicle; the diameter of the heat shield was similarly fixed by the diameter of the launch vehicle at the spacecraft interface. Thus, ballistic coefficients for this class of vehicles have historically tended to be in the range of 2500-5000 Pa.[a]

The ParaShield concept, in summary, involves decoupling the ballistic coefficient from the launch vehicle parameters, to arrive at a vehicle configuration which will provide a value of β which optimizes the desired entry characteristics. As will be shown below, the use of very low values of β results in benign entry conditions, allowing the use of deployable heat shields with reusable ceramic cloth coverings. These same low values of β also result in a very low ($\sim$20 m/sec) terminal velocity, allowing the use of simple impact attenuation to provide a soft landing on water or dry land. Since the same deployable fabric framework serves the functions of both heat shield and parachute, it is referred to as a *ParaShield*.

Even if ParaShield were equally effective in providing for safe entry, descent, and landing (EDL), it is unlikely that there would be any overriding reason to abandon "classical" heat shields and parachutes in favor of the ParaShield, all other things being equal. However, there is another intrinsic advantage of the ParaShield approach: since the heat shield is so much larger than the spacecraft, the physical shape of the spacecraft body is relieved of the requirement to fit within the hypersonic flows of a conformal heat shield. This means that the spacecraft can take the form of a cylinder or other desirable shape, with better internal packing factors and lighter in weight than a traditional conical entry vehicle. Figure 1 shows a concept for a small Explorer-class spacecraft designed for recovery via ParaShield. A further advantage is the ability to articulate the structural interface between the spacecraft and the shield to provide real-time moderation of entry lift/drag ratio, as illustrated in Figure 2.

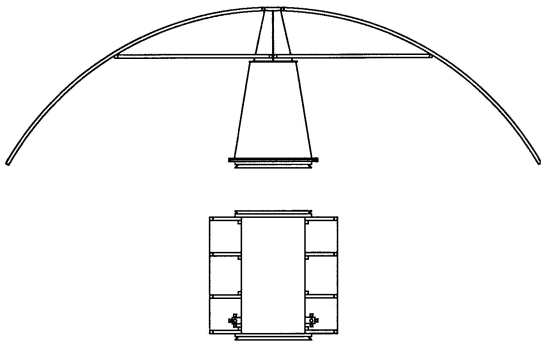

Figure 1. Concept for small orbital ParaShield mission (propulsion module separating following deorbit burn)

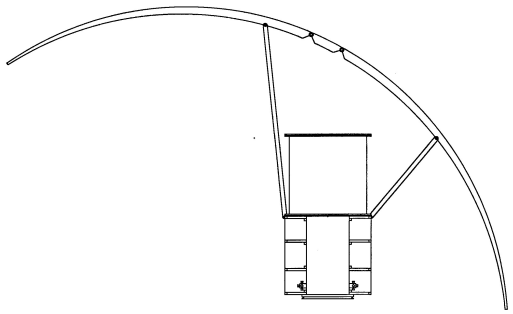

Figure 2. ParaShield payload articulated to control β L/D during entry

[a]Given the definition of β which involves mass and area, the pedantically correct units for this parameter would be kg/m^2. However, in the English system of measurements β is always given in the form of lbs/ft^2; some textbooks introduce a additional term of "g" to the numerator to rationalize the use of units representing weight per unit area. The author, perhaps regrettably, has chosen to use Pascals (or N/m^2) as the assumed dimensional unit of β, as the metric equivalent of lbs/ft^2.

II. Basic Theory

Viewed parametrically, the ballistic coefficient significantly affects the nature of the entry profile, in terms of heating and trajectory. A simulation was written to directly integrate the vehicle state equations for orbital entry, and validated against published data from Viking and shuttle entry dynamics. The simulation included modeling of stagnation point heating rates and temperatures based on the classic Chapman equations.[1]

Figure 3 shows the effect of ballistic coefficient on peak deceleration in a typical low Earth orbit (LEO) entry. As would be expected from traditional entry analysis, β has no first-order effect on deceleration rates; the curves show nearly uniform g levels varying inversely with lift/drag (L/D) ratio. Ballistic coefficient does play a significant role, however, in the maximum stagnation point temperature and maximum heating rates. Figure 4 shows the peak heat shield temperature dropping at an increasing rate as β goes lower and lower; the same trend (if less pronounced) is also seen in peak heating rates in Figure 5. There is also some moderation of these parameters with increasing lift/drag ratio in both cases. In summary, these graphs show a substantially more benign entry environment if the ballistic coefficient of the spacecraft can be reduced below 250 Pa. In comparison, the ballistic coefficient for the Apollo command module was 3500 Pa.[2]

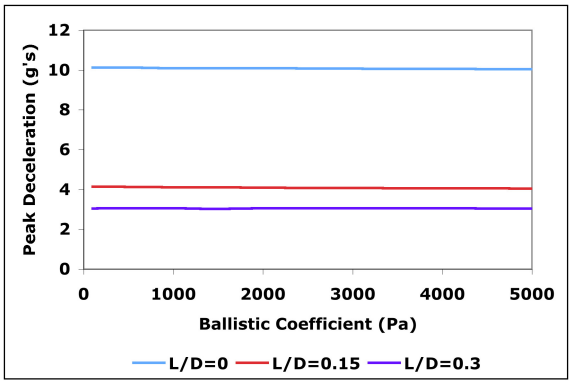

Figure 3. Deceleration loads in LEO entry as a function of ballistic coefficient

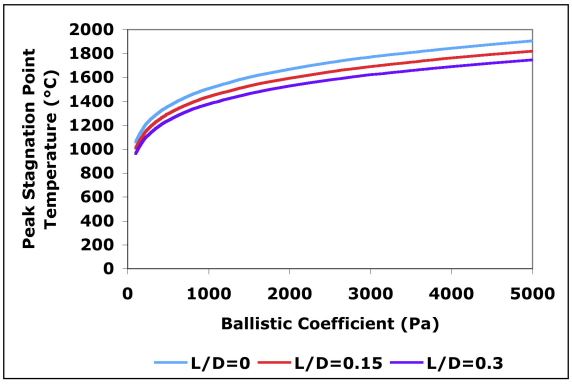

Figure 4. Peak stagnation point temperatures as a function of β

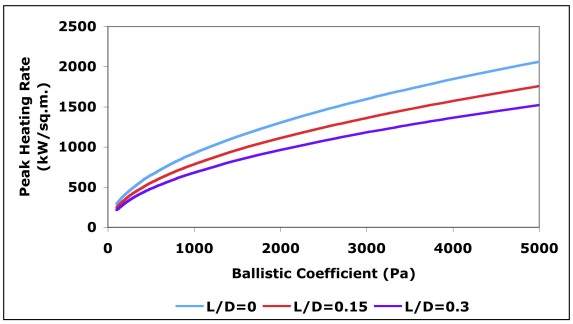

Figure 5. Peak heating rate as a function of β

The fundamental analysis of the ParaShield concept was performed during a graduate design class at M.I.T. in the Fall 1988 term. Given the assignment of developing a human spacecraft to supplement or replace the shuttle flying on the existing expendable launch vehicles of the time (Delta II, Atlas, and Titan IIIC), the ParaShield design lent itself well to the diverse capabilities of the three launch vehicle families. The use of a cylindrical pressure vessel, made feasible by the large ParaShield hypersonic wake, allowed the use of a "stripped-down" two-person version of the spacecraft for a Delta II launch, but the same cabin also permitted a eight-person Titan IIIC mission for space station resupply and crew rotation. This study selected

a desired β of 150 Pa for the vehicle, resulting in peak shield temperatures well within the capabilities of existing off-the-shelf ceramic fabrics such as 3M^{TM} Nextel^{TM} series.[3]

III. Suborbital Test Flight Attempt

In the Spring of 1989, the American Rocket Company (AMROC) contacted the Space Systems Laboratory (then at M.I.T.) about the availability of a flight opportunity on the first flight of their SET-1 launch vehicle. The SSL responded with a design for a ParaShield vehicle optimized for the suborbital trajectory (110 mile apogee, impact 150 miles downrange) of the planned mission. This flight test vehicle, designed and built in a period of five months, was named *Skidbladnir* after an ingenious folding boat of Norse mythology.

The design concept for *Skidbladnir* was a conical pressure vessel, containing all of the vehicle systems, with the ParaShield folded around it for launch. *Skidbladnir* was basically a complete spacecraft, incorporating control systems (redundant microprocessor-based controllers), propulsion system (cold-gas nitrogen thrusters for three-axis stabilization), flight control sensors (three-axis accelerometers and angular rate sensors), data collection system (microprocessor-based solid state data storage for an array of thermal, pressure, and strain gauge sensors), recovery systems (dual radio direction finding beacons, flotation collar, water dye marker, and a high intensity strobe), and payload (two film cameras and a video camera). Limitations of the vehicle, based on the suborbital flight, the constraints of the launch vehicle, and the limited budget and development time included:

- ballistic coefficient of 325 Pa, approximately twice that desirable for orbital entry;
- no inertial measurement unit or external sensors for vehicle attitude, requiring the vehicle to sense the deceleration direction at g onset and perform an attitude maneuver to reach the desired entry attitude;
- no in-flight communications capability.

The stowed and deployed configurations of *Skidbladnir* are shown in Figures 6 and 7, respectively. For the suborbital trajectory of SET-1, the heat sield was made of Beta^{TM} cloth, which is a Teflon^{TM}-impregnated glass fabric used for fireproof applications. The shield was deployed by redundant electric motors, which drove twelve Ti-6Al4V ribs to tension the heat shield fabric. While an aft thermal covering was not needed for this mission (and probably would not be required at all), it was installed due to limitations in the aerodynamic modeling codes used in the design process.[4]

Figure 6. *Skidbladnir* ParaShield stowed in launch configuration

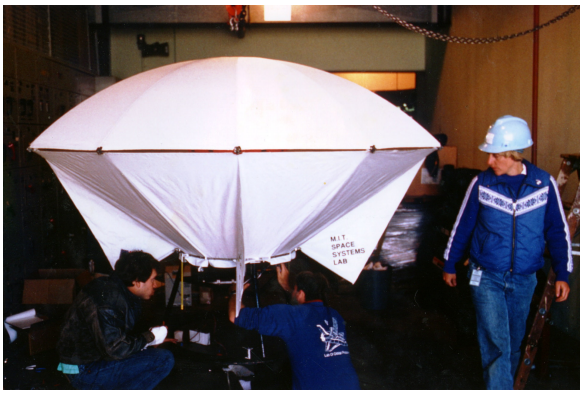

Figure 7. *Skidbladnir* ParaShield in deployed entry configuration

All spacecraft systems functioned nominally during the launch attempt of October 5, 1989, during which the launch vehicle developed insufficient thrust to lift off, was damaged by a fire in the flame deflector, fell over, and burned. Damage to *Skidbladnir* during this incident was limited to a large dent in the capsule and the destruction of the ParaShield ribs and fabric. While disappointing, the overall experience provided an early opportunity to develop a prototype vehicle, and demonstrated the capability of a university laboratory to develop an complete entry vehicle in a very short time, and for an unreasonably small sum of money

($80,000). The *Skidbladnir* spacecraft is currently on display in the University of Maryland (UMd) Space Systems Laboratory, and is available for future flight opportunities.

IV. Experimental Laboratory Testing

The development of the ParaShield concept was highly unusual, in that the concept proceeded immediately to a flight prototype due to a unique launch opportunity, with underlying experimental investigations following. A number of supporting experimental efforts have been performed to validate the fundamental analysis behind the ParaShield concept. Since the greatest unknown lies in the aerodynamics of the exact ParaShield shape, this has been the focus of much of this directed research.

A. Subsonic and Supersonic Wind Tunnel Testing

Initial ParaShield design calculations were based on modified Newtonian flow analysis for a spherical section. However, since the taut fabric will assume a minimum-energy state between physical supports, the flat gores between ribs will most likely have a noticable effect on the aerodynamic characteristics. Another issue was the included angle of the spherical section; while the *Skidbladnir* flight test vehicle's ParaShield approximated a 90^{O} spherical section, that choice was made somewhat arbitrarily, and an experimental effort was initiated to better understand the ParaShield configuration trade space.

A series of wind tunnel tests of ParaShield configurations were performed in subsonic and supersonic regimes. Two-ft. diameter models were made of 12-gored ParaShields with 60^{O}, 90^{O}, and 120^{O} included angles, along with an 90^{O} spherical section. In addition, a 37^{O} conical aft shield structure was created which could be added to any of the ParaShield models to investigate the effects of after-body aerodynamics on lift and drag, as well as stability issues. Figure 8 shows the 90^{O} ParaShield model with aft shroud in the University of Maryland Glenn L. Martin wind tunnel, with smoke being used for flow visualization. Similar tests with 2-in. aluminum models were performed in the UMd Aero Projects Laboratory blow-down supersonic wind tunnel, with Schlieren photography used for flow visualization (Figure 9). Both set-ups included instrumented model stingers for direct measurement of lift, drag, and pitching moments.

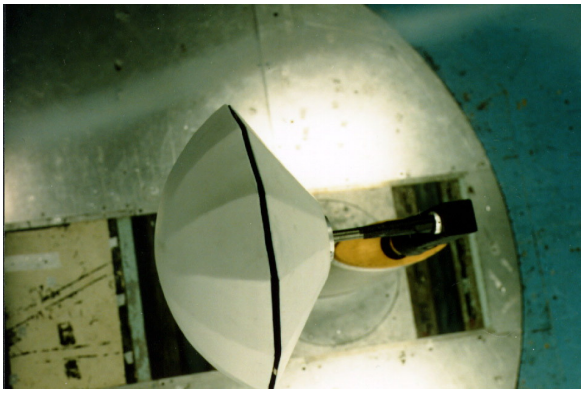

Figure 8. ParaShield model with aft shroud in wind tunnel

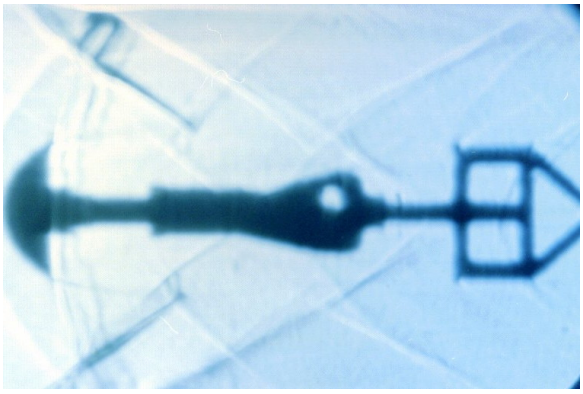

Figure 9. Schlieren photograph of supersonic flow around ParaShield

These tests validated the aerodynamic modeling of the ParaShield in both subsonic and supersonic regimes, and helped to refine performance estimates. The 12-gored panels were acceptably close in performance to an ideal spherical section, and the aft shroud was shown to be unnecessary for both L/D and dynamic stability. Problems with both the 60^{O} and 120^{O} models confirmed the choice of a 90^{O} included angle for nominal ParaShield designs, and verified the design goal of an L/D=0.2 at a 15^{O} angle of attack.[5]

B. Hypersonic Computational Fluid Dynamics

As a complementary effort to the wind tunnel testing, computational fluid dynamics (CFD) was also performed on the ParaShield design. This study looked into the aerothermodynamic environment of a LEO entry, and included analysis of aft wake effects (Figure 10). This work confirmed the supersonic wind tunnel

testing, and went into significant depth on secondary effects such as fabric luffing at the outer edges and the effects of shield porosity to the incoming air flow.

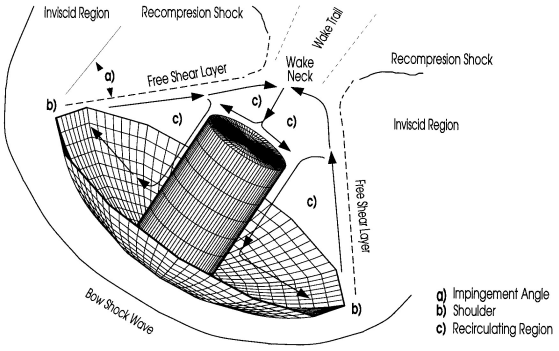

Figure 10. Computational model for flow around ParaShield[6]

Results of this analysis showed that a multilayer Nextel 312 shield could survive LEO entry with a small, but positive thermal margin. The wake angle off the outer shield edge at a 15^{O} angle of attach was analyzed to be 35^{O} with respect to the vehicle axis of symmetry; this would allow the use of spacecraft structures longer than the deployed diameter of the ParaShield without concern for aft wake impingement on the structure. This study also examined a four-rib shield design for feasibility, but concluded that further analysis and probably testing would be required for a ParaShield configuration that deviates to such as great extent from the baseline spherical section.[6]

V. Potential Applications

Systems studies have indicated a variety of useful unmanned applications of ParaShield. Since the mission approach is inherently safe (all recovery devices are locked into place prior to deorbit), routine flights of a commercial sample return vehicle could be made over inhabited areas, resulting in targeted landings at ranges such as White Sands or Edwards Air Force Base. A thousand-kilogram vehicle should have a payload capability on the order of three hundred kilograms; economies of scale yield larger payload fractions for larger vehicles.

The low ballistic coefficient of the ParaShield makes it ideally suited for low-density aerocaptures, such as at Mars. Current plans for a Mars sample return mission involve the use of ballistic Earth entry vehicles without parachutes, since the system would have to be designed to ensure sample quarantine even following a parachute deployment failure. Since the ParaShield can be latched into the deployed configuration days or weeks before Earth encounter on the return trip, there is no post-entry deployment to fail, resulting in a much slower and less stressful landing for the samples. Analyses have been performed for entry velocities up to 16.5 km/sec, typical of the proposed comet nucleus sample return mission. The mechanically-deployed ParaShield system is not susceptible to pressurization failures, as is a ballute, nor is it particularly easy to damage, as are rigid thermal tiles.

Recent mission analyses have focused on the ability of the ParaShield to perform missions planned for the Orion vehicle in the Constellation architecture: ISS crew rotation and direct Earth entry from the Moon. In addition, studies have also been performed on the ability of a ParaShield vehicle to perform direct entry from a Mars return trajectory. In all of the following analyses, the ParaShield is assumed to be a 90^{O} shield with β=200 Pa, flown at a 15^{O} angle of attack to produce an L/D of 0.2. The comparison data shown is for an Apollo Command Module (geometrically identical to Orion), with β=3500 Pa and L/D=0.3. This gives an initial advantage to Apollo/Orion due to the higher L/D value. ParaShield entry flight path angles are not constrained to the historical Apollo values, but have been optimized for the ParaShield flight parameters.

A. International Space Station Resupply and Crew Rotation

The initial planned Orion application was to resupply crew to the International Space Station. The entry trajectory for this mission was calculated as an elliptical orbit tangent at apogee to the ISS orbit, and reaching atmospheric interface altitude at the desired flight path angle. Figure 11 shows the entry trajectories for the baseline ParaShield and Apollo spacecraft . The ParaShield vehicle, being lighter, lofts earlier and lands shorter than the Apollo-class vehicle. Figure 12 shows the same trajectory in terms of velocity vs. altitude. This graph clearly shows that the lighter ParaShield dissipates its kinetic energy higher in the atmosphere, and arrives at a significantly lower terminal velocity than Apollo.

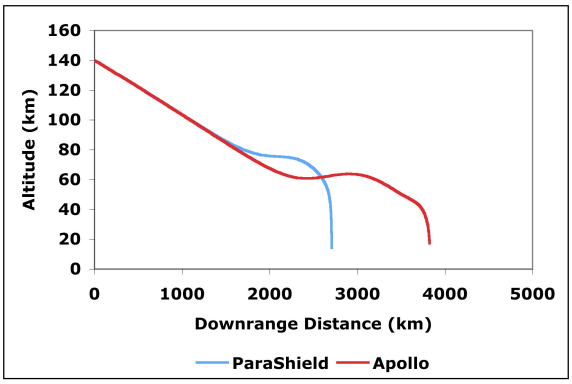

Figure 11. Entry trajectories for Apollo and ParaShield spacecraft from ISS orbit

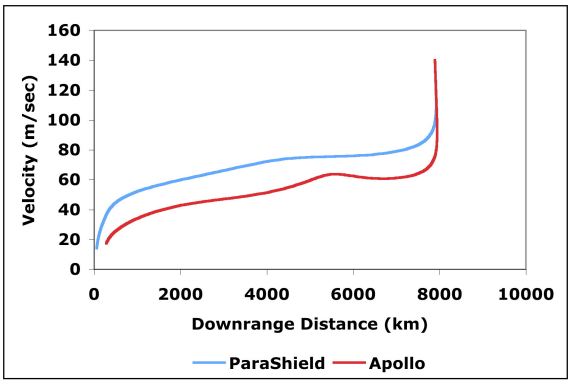

Figure 12. Time histories of velocity profiles in ISS entry

Figure 13 plots the vehicle decelerations against time since atmospheric entry. The entry flightpath angle for ParaShield was chosen to keep the maximum deceleration levels comparable to Apollo. Due to the assumed lower L/D of the ParaShield, its crew has to endure a longer high-g impulse, but the total deceleration period is slightly shorter for its lower areal loading. Both of these deceleration profiles should be acceptable for spacecraft whose human occupants are returning from prolonged exposure to microgravity.

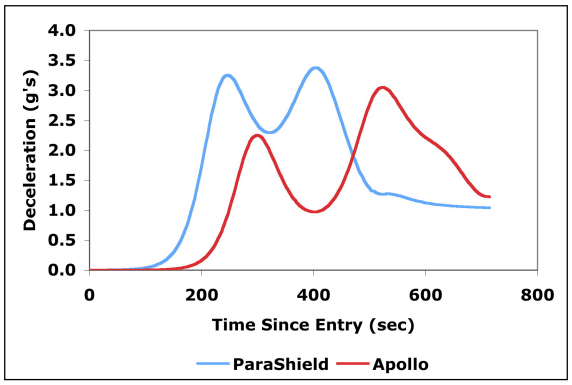

Figure 13. Deceleration loads on Apollo and ParaShield vehicles in LEO entry

Thermal data on the ParaShield is presented in the next two charts. The time profile of the stagnation point temperature (Figure 14) shows a marked decrease from Apollo to ParaShield, with peak temperature for the latter only reaching 800^{o}C. Similarly, the maximum heating rates (Figure 15) illustrate a five-fold decrease in peak value from the Apollo spacecraft to the ParaShield.

Overall, the comparative analysis demonstrates that a ParaShield vehicle can do the same mission as an Apollo-class spacecraft for entry, descent, and landing from an ISS crew rotation mission. The advantage of ParaShield for this application is the greater protected volume behind the shield; the Apollo-equivalent vehicle could easily support a Mini Pressurized Logistics Module (MPLM) for rotation of up to 1800 kg of crew and/or cargo. Unlike Soyuz, Apollo, or Orion, the ParaShield ISS vehicle would provide substantial

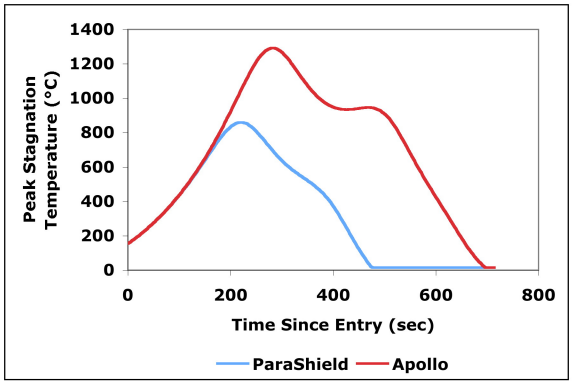

Figure 14. Stagnation point temperature profiles during LEO entry

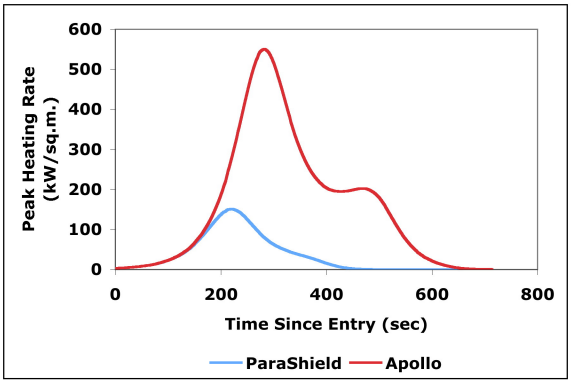

Figure 15. Maximum heating rates in LEO entry

pressurized downmass, allowing ISS maintenance and logistics to proceed on the original basis of planned equipment return for ground servicing and reuse,, rather than the "use it up/burn it up" mode required without substantial downmass for cargo.

B. Human Lunar Exploration

Just as Orion was planned to support both ISS crew rotation and human lunar exploration missions, it would be important for the ParaShield vehicle to also support direct Earth EDL from the lunar return trajectory. For this purpose, the trajectory simulation code was used to investigate entry characteristics for Apollo and ParaShield vehicles performing a hypervelocity entry (11 km/sec) from the Moon.

The basic lunar entry trajectory is shown in Figure 16. Unlike the orbital entry simulation, which used a constant upwards lift vector throughout the entry profile, the hypervelocity entries required lift moderation to keep from "skipping out" of the atmosphere or from entering too steeply. The entry vehicle roll orientations were varied between 0^{O} (lift vector upwards) and 180^{O} (lift vector downwards) to approximate an equilibrium glide entry. The trajectories follow the trends of the orbital entry case, with the ParaShield vehicle lofting higher earlier in the trajectory, and landing approximately 500 km farther uprange than the Apollo baseline vehicle. Figure 17 shows the trends with velocity as a function of altitude; the rough nature of these curves is illustrative of the quantization of the vehicle roll control and the vestiges of natural phugoid motion.

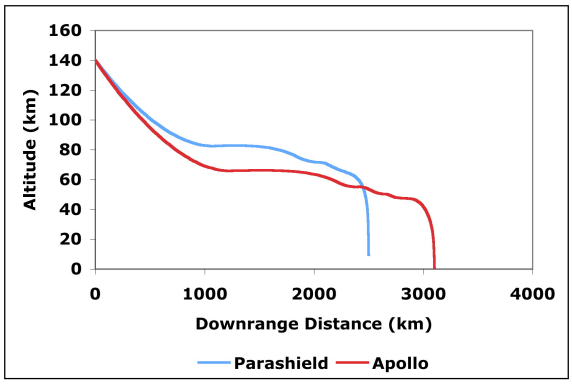

Figure 16. Entry trajectories for Apollo and ParaShield spacecraft in direct lunar return trajectory

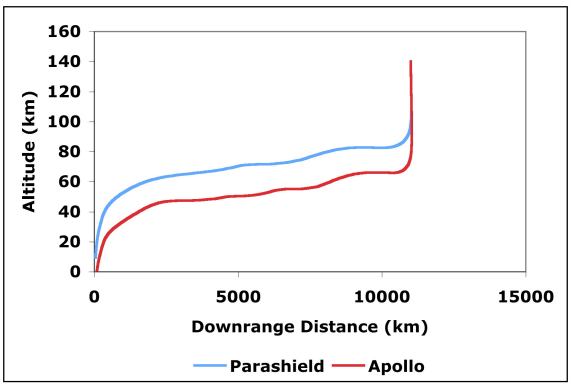

Figure 17. Time histories of velocity profiles in lunar entry

The comparative deceleration curves are shown in Figure 18. Even with the difference in L/D between the two vehicles, these curves illustrate how closely the ParaShield trajectory can be controlled to model the baseline Apollo entry. Both vehicles top out at approximately 6 g's on entry.

Figure 19 shows the stagnation point temperatures during entry. With the higher entry velocity from the lunar return orbit, the heat shield temperatures are elevated over the orbital entry case in Figure 14.

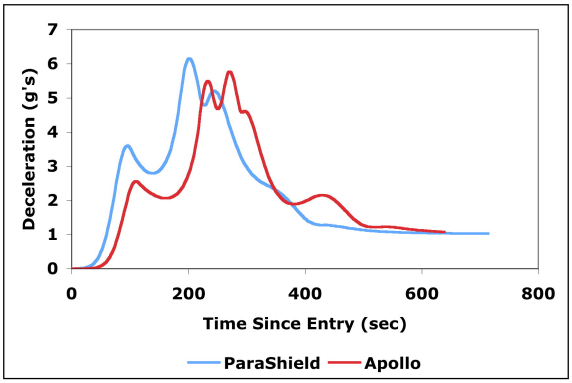

Figure 18. Deceleration loads on Apollo and ParaShield vehicles in lunar entry

The ParaShield temperature tops out at approximately 1100^{O}C, which is near the upper limit for off-the-shelf ceramic fabrics currently. Figure 20 shows that the higher-energy entry has an even larger discrepency between the classical and ParaShield heat flux, with the ParaShield material exposed to an order of magnitude less heating rate than the Apollo-style heat shield.

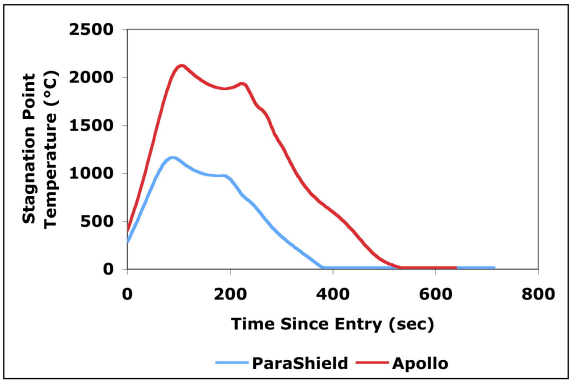

Figure 19. Stagnation point temperature profiles during lunar entry

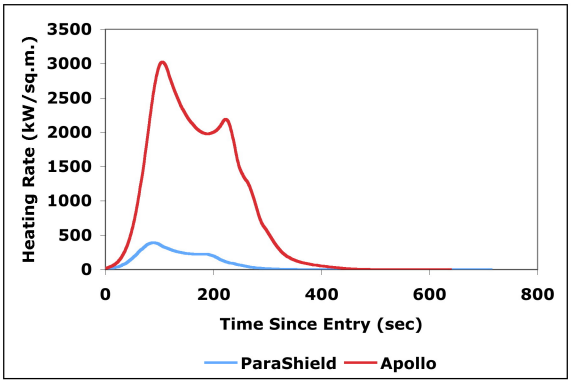

Figure 20. Maximum heating rates in lunar entry

Again, this analysis demonstrates that the ParaShield vehicle can equal the Apollo-class vehicle in performing a human-compatible direct entry from the lunar return trajectory. The main benefit for the ParaShield vehicle in this case accrues only if the mission architecture is allowed to exploit the ParaShield advantages. No space vehicle is as expensive to develop, on a per kilogram basis, than a human-carrying spacecraft. For a lunar-orbital rendezvous architecture such as Apollo or Constellation, two such vehicles have to be developed: the lunar landing and ascent vehicle, and the Earth return vehicle. Due to the relaxed constraints of the ParaShield EDL system, one can envision a single crew capsule which works for both the launch and entry phases, and is transferred to a landing vehicle for the lunar descent and ascent. The ParaShield, as an integrated EDL system, can be detached and left in orbit, providing a more closely optimized human spacecraft for each phase of the mission.

C. Human Mars Exploration

It is also interesting to look ahead, and examine the utility of a ParaShield system for direct Earth entry following a return from Mars. This would result in an entry velocity of about 12.5 km/sec, for most trajectory options under consideration. Since this is not a mission for which Apollo (or, for that matter, Constellation) was designed, the feasibility study here will only examine the ParaShield vehicle, again at a β of 200 Pa. Figures 21 and 22 show the trajectory information for this entry. The form is similar to that for the lunar

entry, although the higher entry velocity from Mars results in deceleration at a higher altitude, and a longer total travel downrange to the landing point.

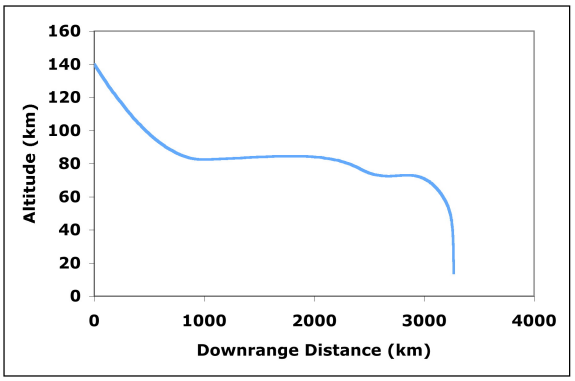

Figure 21. Entry trajectories for Apollo and ParaShield spacecraft in direct Mars return trajectory

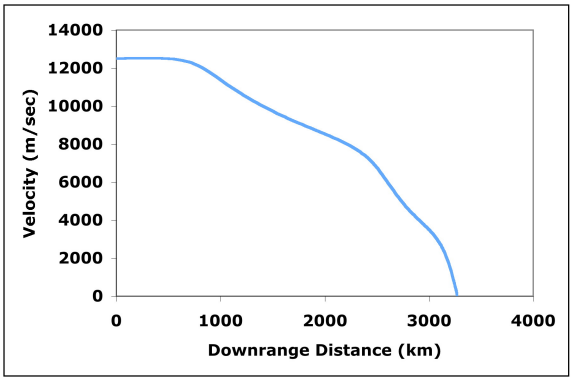

Figure 22. Time histories of velocity profiles in Mars entry

Figure 23 shows the deceleration rates during Mars entry. As in the lunar case, the vehicle roll vector is actively oriented to tailor the entry profile and maintain a 5 g upper limit for the crew. This results in three deceleration peaks over the first seven minutes of the entry, none of which exceed the target limit.

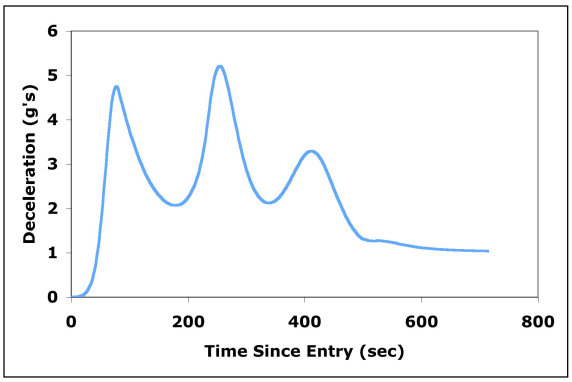

Figure 23. Deceleration loads on Apollo and ParaShield vehicles in Mars entry

The thermal data on Mars entry are shown in Figures 24 and 25. As expected, the higher velocity entry translates to higher temperatures and higher heating rates. The peak ParaShield temperature of 1300^{O}C will require higher temperature ceramic fabrics than the LEO and lunar entry cases. The peak heating rate of 600 kW/m^2 is more than twice that of lunar ParaShield entry and five times that of LEO entry; interestingly enough, it is approximately the same heat flux (in both peak and profile) as an Apollo spacecraft performing an LEO entry.

It is not until we reach a Mars entry case that the ParaShield vehicle presents a technology challenge due to limitations of present-day materials. Again, the expectation is that a ParaShield EDL system for Earth return would provide synergy through the reuse of crew cabins for both interplanetary cruise and Mars landing and ascent. It would be interesting to examine the utility of ParaShield technology for Mars EDL, but this will left for a future paper that more fully examines the detailed implications of ParaShield in a Mars exploration architecture.

VI. Conclusions and Future Research

Concepts for ultra-low ballistic coefficient entry vehicles date back at least to 1959 and the Avco proposal for a Mercury spacecraft with a deployable heat shield of titanium shingles.[7] Recent approaches to this

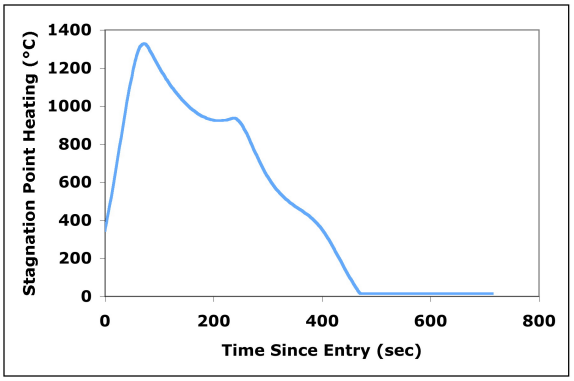

Figure 24. Stagnation point temperature profiles during Mars entry

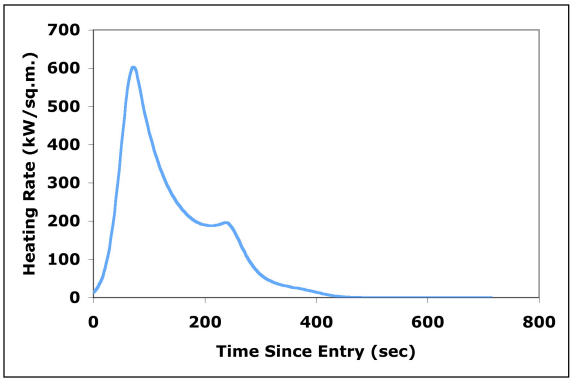

Figure 25. Maximum heating rates in Mars entry

concept have focused on inflatables, both in the United State[8] and Europe.[9] Both of these systems flew ballistic trajectories using inflatable structures to lower the ballistic coefficient of the system. The U.S. Inflatable Reentry Vehicle Experiment was a subscale vehicle flown on a sounding rocket. The three European Inflatable Reentry and Descent Technology test flights attempted orbital descents, although only one was partially successful. In addition, the IRDT spacecraft was approximately the same size as the *Skidbladnir* spacecraft, while heavier than designs for a corresponding orbital ParaShield vehicle and with a smaller payload mass fraction.

Whether inflatable or mechanically deployed, ULβ entry vehicles offer the advantages of

- large protected volumes free of aft wake impingement for accommodation of arbitrary payload shapes, including cylindrical pressure vessels with better packing efficiencies than traditional conical entry vehicles,
- lower enthalpies in entry, for enhanced communications and navigation throughout the entry trajectory, and
- innovative integration of EDL systems with spacecraft, since the heat shield is deployed rather than fixed throughout flight.

Beyond these advantages inherent in ULβ systems, the further benefits of the ParaShield concept over inflatables include

- mechanical system to deploy and lock the shield, which does not require power or pressurization to support the external shape once established,
- the rigid shield structure allows the use of center of mass offset to create moderate lift/drag ratios, which in turn provide lower g-loadings and the ability to control the lift vector to increase landing accuracy, and
- the entire payload is protected behind the shield, which is capable of supporting full stagnation point heating throughout entry.

Future efforts to verify and validate the potentials of the ParaShield concept should include additional systems studies, dynamic analysis of vehicle stability throughout the flight profile, and experiments into innovative packaging and deployment mechanisms for the potential range of ParaShield sizes. Ultimately, the system needs to be validated through flight testing. While initial tests in suborbital flight would provide corroboration of the concept, ultimately the goal should be a low-cost orbital EDL experiment. Conceptual designs have been created in the SSL for small-scale ParaShield orbital flight test vehicles compatible with the EELV secondary payload adapter (ESPA) ring, which would allow orbital access at reasonable costs.

Acknowledgements

The author would like to thank all those who have worked on various aspects of the ParaShield project down through the years. Specifically, I would like to acknowledge Dr. Russell Howard, Jud Hedgecock, and Rich Patton for their innovative work in the original design class which created the ParaShield concept, as well as all of their volunteer work in designing, fabricating, integrating, and operating the *Skidbladnir* spacecraft for the attempted suborbital flight test. I would also like to thank Dr. Robert Wolf, who arranged the flight test opportunity at the American Rocket Company. Dennis Loveless performed the subsonic and supersonic wind tunnel testing, and Harry Magazu, under the capable supervision of Dr. Mark Lewis, performed the CFD analysis; all of their efforts are gratefully appreciated.

References

[1]Dean R. Chapman, "An Approximate Analytical Method for Studying Entry into Planetary Atmospheres" NASA TR-R-11, 1959

[2]Jeffrey S. Robinson and Kathryn E. Wurster, "Trajectory and Aeroheating Environment Development and Sensitivity Analysis for Capsule-Shaped Vehicles" AIAA-2006-7949, *14th AIAA/AHI International Space Planes and Hypersonics Systems and Technologies Conference*, Canberra, Australia, November 2006

[3]R. Patten and J. Hedgecock, "A Novel Approach to Spacecraft Re-entry and Recovery", SSL Report 8-89, 1989

[4]David L. Akin, "The ParaShield Entry Vehicle Concept: Basic Theory and Flight Test Development", *4th Annual USU/AIAA Small Satellite Symposium*, Logan, Utah, August 1990

[5]Dennis L. Loveless II, "Subsonic and Supersonic WInd Tunnel Evaluation of Ultra Low Ballistic Coefficient Entry" M. S. Thesis, Department of Aerospace Engineering, University of Maryland, 1994

[6]H. K. Magazu, M. J. Lewis, and D. L. Akin, "Aerothemodynamics of a ParaShield Re-Entry Vehicle" *AIAA Journal of Spacecraft and Rockets*, Vol. 35 No. 4, pp. 434-441

[7]R. W. Detra, A. R. Kantrowitz, F. R. Riddel, and P. H. Rose, "The Drag Brake Manned Satellite System", Research Report #64, AVCO-Everett Research Laboratories, Everett, MA, August 1959.

[8]Stephen J. Hughes, Robert A. Dillman, Brett R. Starr, Ryan A. Stephan, Michael C. Lindell, Charles J. Player, and F. McNeil Cheatwood, "Inflatable Re-Entry Vehicle Experiment (IRVE) Design Overview", AIAA-2005-1636, *18th AIAA Aerodynamic Decelerator Systems Technology Conference and Seminar*, Munich, Germany, May 2005

[9]Detlev Wilde, Stephan Walther, Konstantin Pitchadze, Sergej Alexsaschkin, Dietrich Vennemann, and Lionel Marraffa, "Inflatable Reentry and Descent Technology (IRDT) - Further Developments" *2nd International Symposium on Atmospheric Reentry Vehicles and Systems*, Archchon, France, March 2001